Three-dimensional bimodal buoyant flow transitions in tilted enclosures

H. Q. Yang and K. T. Yang
Department of Aerospace and Mechanical Engineering, University of Notre Dame, Notre Dame, IN 46556, USA

and J. R. Lloyd
Department of Mechanical Engineering, Michigan State University, East Lansing, MI 48824, USA

Received 26 February 1987 and accepted for publication 1 June 1987

A numerical study has been conducted to track laminar flow transitions and heat transfer characteristics in tilted three-dimensional rectangular enclosures with square differentially heated side surfaces. The bimodal flow patterns for the heated-from-below case are found to be very stable and insensitive to changes in the aspect ratios and Rayleigh numbers. Tilt of the enclosure produces a complicated three-dimensional transition which can be viewed as the combination of transitions found in transverse and longitudinal enclosures. A local minimum heat transfer has been found at a critical angle which corresponds to the transition of three-dimensional complicated flow to a unicell.

Keywords: three-dimensional flow; natural convection; inclined enclosures

Introduction

Important applications of natural convection in tilted enclosures (Figure 1) have made it an active research area in recent times. Much of this effort has been directed toward transverse enclosures for which the aspect ratio $A_z(L/H)$ is much larger than the aspect ratio $A_x(W/H)$. The primary reason is that two-dimensional flow prevails as long as the tilt angle is such that three-dimensional flow transition does not occur. Such phenomena can be modeled numerically by simple two-dimensional models and various effects such as boundary conditions, tilt angles, internal heat sources, and internal baffles can be determined without much difficulty.[1-3] However, in many physical instances, buoyant enclosure flows are predominantly three-dimensional, caused either by the specific geometries involved or by the nature of prescribed boundary conditions. Unfortunately, our current understanding of such flows is still somewhat limited,[3,4] and the purpose of this study is to provide additional insight into three-dimensional flow transitions in tilted enclosures as affected by enclosure geometry in our continuing studies in this area.[5,6]

It is well known that the tilt of the enclosure greatly affects the flow patterns and heat transfer because of changing controlling mechanisms. In general, the hydrodynamic effect in the vertical heated-sidewall position gives a two-dimensional unicell which aligns its axis perpendicular to the plane of the gravitational vector **g** and temperature gradient $\mathbf{\Delta T}$, whereas the thermal instability effect in the heated-from-below position will result in a set of two-dimensional multicell structures aligning their axes in the short geometry direction, once the Rayleigh number exceeds a critical value $\mathrm{Ra_c}$. In the latter case, the gravitational vector **g** is parallel to that of the temperature gradient. It can be expected, therefore, that different flow transitions will be possible, depending on different physical geometries. As experimentally observed in Refs. 7–9 and numerically verified[5,10] for a transverse enclosure, the flow changes from a two-dimensional unicell in the x-y plane to a two-dimensional multicell structure in the y-z plane with a right-angle change in the cell axes. The heat transfer rate undergoes a local minimum at a critical angle ψ_c which lies between 90° and 180°, as the enclosure is tilted from the vertical position (90°) to the horizontal position (180°) (Figure 2).

In an earlier paper[5] the flow transitions and heat transfer characteristics in the tilted transverse enclosure for the entire range of angles, including the angles at which the three-dimensional flow transitions take place, have been calculated by using several numerical models (roll-cell model, full 3-D model, and 2-D model) based on the QUICK scheme. Good comparisons with experimental data have been found, and a local minimum in the heat transfer rate is shown to correspond

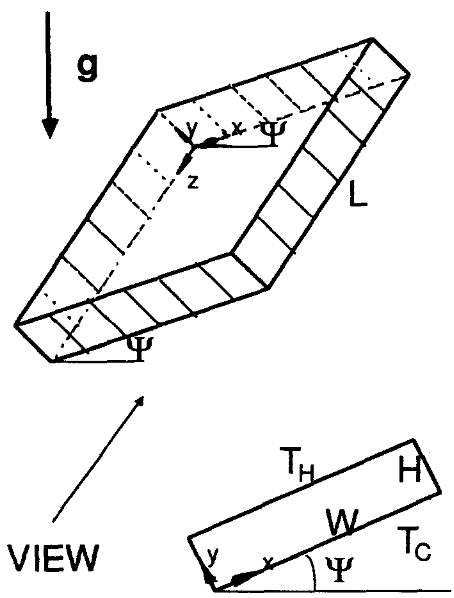

Figure 1 Three-dimensional rectangular enclosure geometry

to a dramatic change of flow patterns from a 2-D unicell to one with a 2-D multicell with cell axes perpendicular to each other. To slow down the transition process, a transient calculation has been performed, which shows many interesting details of the flow transition process in the neighborhood of the critical angle. In the continuing study[6] three-dimensional numerical callations have been carried out to determine flow transition and heat transfer characteristics in tilted three-dimensional rectangular differentially heated longitudinal enclosures for which the aspect ratio A_z is much less than the aspect ratio A_x (see Figure 3). It is found that there also exists a local minimum in the heat transfer rate (like the transverse enclosure) corresponding to the transition of flow from unicell to multicell structures, but the transition is in the same plane (unlike the transverse enclosure). This agrees very well with existing experimental data and observations.[11] Simulation calculations with different A_z show that the close proximity between the lateral walls restricts the flow development in that direction, thus reducing the overall heat transfer across the enclosure.

Thus, the flow transition and heat transfer characteristics in tilted transverse and longitudinal enclosures have now been clarified, and it is only natural to inquire about the same characteristics for A_z equal to A_x. Such cases may be referred to as bimodal flow, related to the heated-from-below situation when the bottom and upper surfaces are squares ($A_z = A_x$), because it is the combination of two sets of perpendicular roll-cells.[12] To our knowledge there are no theoretical or experimental studies on bimodal transition. The objective in the present study is to determine the special properties of bimodal transition at different A_x ($A_z = A_x$) and tilt angles, and their relations to transitions in transverse and longitudinal enclosures.

Mathematical modeling

The problem considered here is steady laminar natural convection in a tilted rectangular box enclosure with four adiabatic surfaces and two differentially heated opposite square surfaces (T_H and T_C, respectively). The enclosure is tilted along the z-axis. The tilt angle ψ is 180° with T_H at the bottom surface, and it becomes 0° for the heated-from-above situation (see Figure 1). The phenomena can be modeled by the following conservation equations:

$$\rho_t + (\rho u_i)_{,i} = 0 \tag{1}$$

$$(\rho u_i)_t + (\rho u_i u_j)_{,j} = -p_{,i} - \rho g_i + \sigma_{ij,j} \tag{2}$$

$$(\rho c_{pm} T)_t + (\rho u_i c_{pm} T)_{i,} = (k T_{,i})_{,i} + \mu \Phi - p u_{i,i} \tag{3}$$

The shear stress tensor σ_{ij} is

$$\sigma_{ij} = \mu(u_{i,j} + u_{j,i} - \tfrac{2}{3}\delta_{ij} u_{k,k}) \tag{4}$$

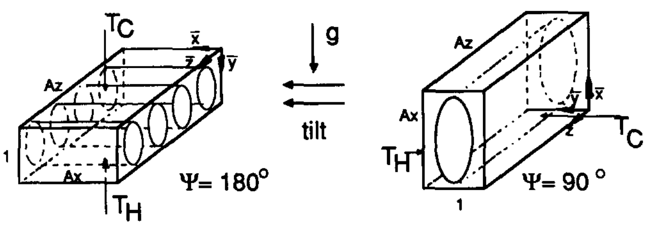

Figure 2 Transverse enclosure and its transition

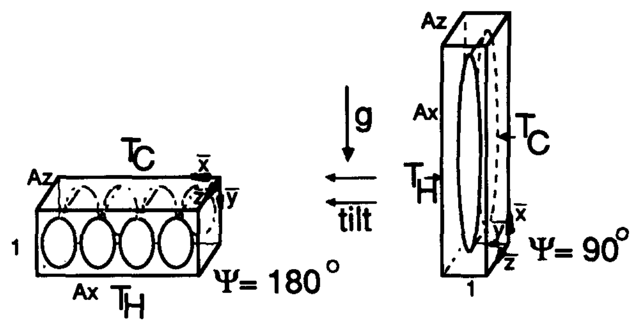

Figure 3 Longitudinal enclosure and its transition

Notation

A_x	Aspect ratio W/H
A_z	Aspect ratio L/H
B_x, B_y	Parameters for coordinate transformation
c_p	Isobaric specific heat
c_{pm}	Mean specific heat
g_i	Gravitational acceleration vector, $i=1, 2, 3$
H	Height of enclosure
h	Coefficient of heat transfer
k	Thermal conductivity
L	Length of enclosure
Nu	Nusselt number hH/k
p	Static pressure
Ra	Rayleigh number, $\rho g \beta (T_H - T_C) H^3 / \mu_R \alpha_R$
T	Temperature
u_i	Velocity components, $i=1,2,3$
W	Width of enclosure
x, y, z	Rectangular coordinates
x^*, y^*	Transformed coordinates

Greek symbols

α	Thermal diffusivity
β	Volume expansion coefficient
$\Delta x, \Delta y, \Delta z$	Calculation cell sizes
δ_{ij}	Kronecker delta
μ	Dynamic viscosity
ρ	Density
σ_{ij}	Shear stress tensor
Φ	Dissipation function
ψ	Tilt angle
ψ_c	Critical tilt angle

Superscript

$\bar{}$	Dimensionless coordinate normalized with H

Subscripts

C	Cold wall
H	Hot wall
i, j, k	Coordinate indices
R	Reference quantities
t	Time derivative
m	Mean quantities

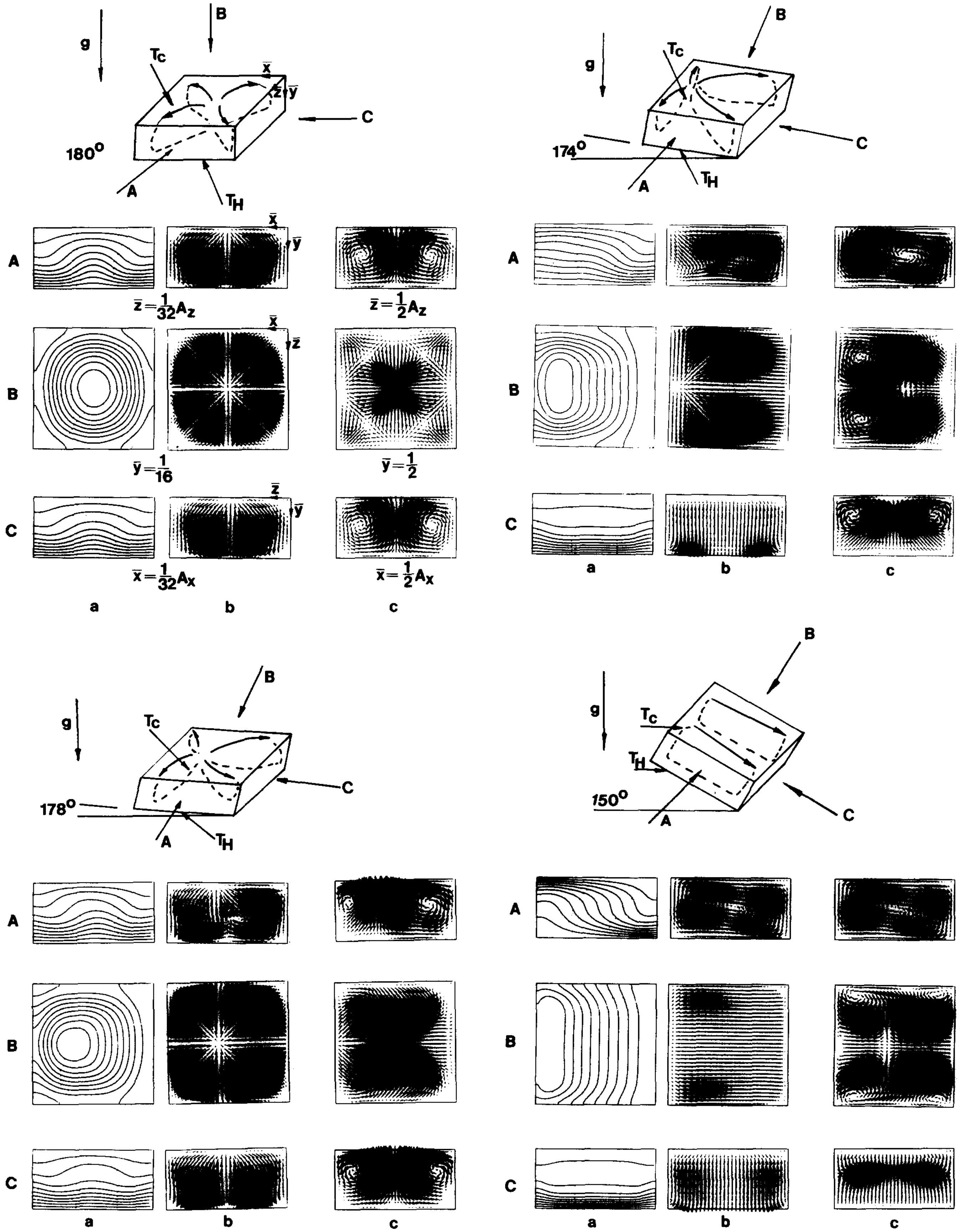

Figure 4 Isotherms a and flow patterns b, c in a tilted square box of $A_x=A_z=2.0$ and Ra$=8\times10^3$: (a)$\psi=180°$; (b) $\psi=178°$; (c) $\psi=174°$; (d) $\psi=150°$

the mean specific heat is

$$c_{pm} = \frac{1}{T - T_C} \int_{T_C}^{T} c_p(T)\,dT \qquad (5)$$

and the dissipation function is

$$\Phi = 2(u_{i,j}^2)\delta_{ij} + [u_{i,j}(1-\delta_{ij})]^2 - \tfrac{2}{3}(u_{i,i})^2 \qquad (6)$$

All symbols are given in the notation.

The numerical solution technique by finite differences has been described and discussed in Refs. 5 and 6 and will not be repeated here. Basically, the physical properties μ, k, and c_p are taken to be temperature dependent and are nondimensionalized by their values evaluated at the temperature of the cold wall, respectively. The reference values used for nondimensionalization for T, u_i, and x_i are T_C, u_R (30.48 cm/s) and H, the distance between hot and cold walls. Here T_C, the temperature at the cold wall, is taken as 288.16 K, and T_H, the temperature at the hot wall, is determined from the dimensionless temperature ratio $(T_H - T_C)/T_C$, which is taken to be 0.2 in all the calculations. The quantitative effect of variable physical properties on buoyant enclosure flows has been given in Ref. 3. The fluid medium in the present calculations is air with a Prandtl number of 0.71, and the Rayleigh number is taken to be 8×10^3, which facilitates comparison with known results in the literature. Calculations are based on primitive variables, and discretization is by the control volume approach. The convective terms are represented by the 3-D QUICK scheme which is an extension of those given originally by Leonard.[13] A semi-implicit scheme is used, and all the final difference equations are solved by an iterative tridiagonal matrix solver. All calculations have been carried out on an IBM 3033 mainframe computer. In general, one hour of CPU time accommodates approximately 300 dimensionless time steps, and 2000 time steps are normally needed to achieve steady-state results.

In general, grid refinement studies for three-dimensional problems involving Navier-Stokes equations are difficult because of the usually limited computer storage and excessive CPU time required. In the present study, a grid refinement investigation has been carried out based on a simple pseudo-two-dimensional enclosure problem dealing with a square vertical enclosure with $A_x = A_z = 1.0$ and $\psi = 90°$, and the lateral walls at $z/H = 0$ and 1.0 maintained drag free and adiabatic.[14] A nonuniform grid based on the following coordinate transformations is utilized:

$$x^* = 0.5\,\frac{1 - \exp(xB_x/H)}{1 - \exp(0.5B_x)} \qquad 0 \leqslant \frac{x}{H} \leqslant 0.5 \qquad (7)$$

$$y^* = 0.5\,\frac{1 - \exp(yB_y/H)}{1 - \exp(0.5B_y)} \qquad 0 \leqslant \frac{y}{H} \leqslant 0.5 \qquad (8)$$

which for $B_x, B_y > 0$ automatically place more grid points in the boundary regions where large gradients occur. The uniform grid is recovered with $B_x, B_y = 0$. When the parameters B_x and B_y are large, very fine grids are located near the boundary, and coarse grids are located in the center of the enclosure. Calculations for the pseudo-two-dimensional problem have been carried out for Rayleigh numbers up to 10^7 and sufficiently large values of B_x and B_y to achieve grid-independent results. It has been found that for $\mathrm{Ra} = 10^7$ B_x and B_y must exceed 7.0; for $\mathrm{Ra} = 10^6$, B_x, $B_y > 5.0$; for $\mathrm{Ra} = 10^5$, B_x, $B_y > 3.0$; and for $\mathrm{Ra} \leqslant 10^4$, B_x, $B_y > 0$. This last result indicates that for $\mathrm{Ra} < 10^4$, a uniform grid system is capable of giving grid-independent results. Since the Rayleigh number dealt with in this study is 8×10^3, uniform grid systems have been used in all calculations. Reference 14 also includes other validation studies to insure the accuracy of the calculation results.

Results and discussions

Bimodal flow with $A_x = A_z = 2.0$

The calculation is based on a Rayleigh number of 8×10^3 and started with a linear temperature profile between hot and cold walls and a stagnant fluid field. A grid of $n_x \times n_y \times n_z = 32 \times 16 \times 32$ is adopted, so that $\Delta x = \Delta y = \Delta z = \frac{1}{16}H$. Flows in different planes and streak lines (the path of fluid particles) are shown in Figure 4(a). View A is in the x-y plane along the z-axis at $z = \frac{1}{16}H$ (near wall) and $z = H$ (center). View B is in the z-x plane along the y-axis at $y = \frac{1}{16}H$ (near wall) and $y = \frac{1}{2}H$ (center). Similarly, view C is in the y-z plane along the x-axis at $x = \frac{1}{16}H$ (near wall) and $x = \frac{1}{2}H$ (center).

The three-dimensional flow field is very similar to that observed experimentally by Stork and Müller[12] at Rayleigh numbers around the critical value (3×10^3). Basically, it is a combination of two horizontal roll-cells with axes parallel to the x-axis and another two horizontal ones with axes parallel to the z-axis, resulting in four individual cubic diagonal roll-cells with axes inclined 45° and 135° to the x-axis, respectively. This diagonal roll-cell is similar to that calculated by Ozoe *et al.*[15] with a cubic box heated from below, but initiated with two instantaneous hot and cold elements which are located antisymmetrically with respect to the half height plane ($y = \frac{1}{2}H$ plane). Similar diagonal roll-cells have also been obtained numerically by Chan and Banerjee[16] with a cubic box heated from below. The fluid ascends in the central region and descends near the lateral walls. The formation of this type of motion can be explained as follows: when the fluid near the bottom hot surface is heated, a thermal instability force is generated. This force, which is uniformly distributed with respect to the x- and z-dimensions because of the symmetry of the geometry, attempts to push up all the lighter fluid. However, viscous shear near the lateral wall resists this motion, such that the only way the lighter fluid can move freely is in the central region, once the thermal instability force is sufficiently large ($\mathrm{Ra} > \mathrm{Ra_C}$). To conserve mass, the cooled heavier fluid descends along the lateral walls.

One set of calculations has been carried out to determine the stability of this flow configuration. These calculations start with this flow model as the initial conditions by either increasing or decreasing the temperature difference. This symmetrical cell system is found to be very stable and insensitive to the change of temperatures, except that the velocities are proportionally different. This observation also matches with that observed in the experiment.[12] The Nusselt number in this case is 1.96. Ozoe *et al.*[15] have carried out the calculations of the heated-from-below case for $\mathrm{Pr} = 10$ and $\mathrm{Ra} = 8 \times 10^3$ with three geometrical configurations: (1) cubic box, (2) infinite horizontal plate, and (3) long channel with square cross section. The resulting Nusselt numbers are 1.746, 2.617, and 2.482, respectively. According to Ref. 15 these data are expected to provide a good approximation for all $\mathrm{Pr} > 1.0$. Considering the difference in the Pr number (1.0 with 0.72) and the grid number (8 with 16), our Nusselt number agrees closely with theirs, because as a result of the influence of the lateral walls it should be higher than that of the cubic box and lower than that of the infinite horizontal plates.

Beginning with this stable model the enclosure is tilted to 178° (heated surface 2° from horizontal). The flow pattern is depicted in Figure 4(b). The symmetry with respect to $x = H$ (center) is somewhat lost because of the presence of the hydrodynamic force along the lateral walls. However, it is still symmetrical with respect to $z = H$ since it has no preferred direction along the z-axis. From view A, which is equivalent to the longitudinal

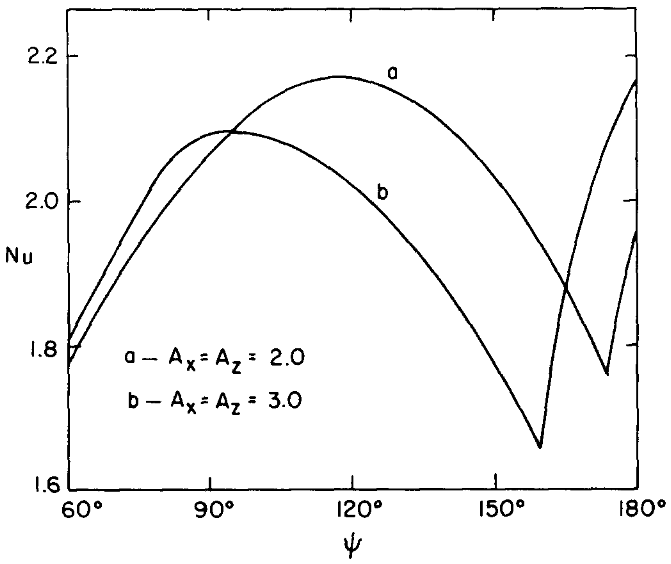

Figure 5 Effect of tilt angle on Nusselt number

enclosure case, the cell far from the z-axis is constrained because of an opposing gravitational force. This force aids the heated fluid at the bottom to flow along the positive x-direction (upslope direction), such that the cell near the z-axis becomes elongated. From view B, the top view, the center fluid moves up. As a result, the center of the two cells in view C separates, which is equivalent to the transverse enclosure. Basically, there are still four "diagonal" roll-cells, but they are rectangular and the circulation axes of roll-cells are no longer at 45° and 135° with respect to the x-axis.

As the enclosure is further tilted to 174° (see Figure 4(c)), the cell in view A, which is constrained at 178°, is almost washed out, and meanwhile the two cells in view C vanish near the wall to accomplish the formation of the unicell in the x-y plane. However, the ones near $x = 2H$ are still vigorous, so the whole flow field looks like two "diagonal" roll-cells. Shown in Figure 4(d) are the results for $\psi = 150°$. Here the transition from a multicellular motion to a unicell with axis parallel to the z-axis is essentially completed; the whole field is almost two-dimensional except in the vicinity of the $z = 0$ and $z = 2H$ lateral walls, where the viscous shear still persists resulting in some three-dimensionality. It is found that beyond this angle the flow is nearly two-dimensional.

Curve a in Figure 5 is the variation of the corresponding Nusselt numbers as a function of the tilt angle. Similar to tilted tranverse[5] and longitudinal[6] enclosures, the characteristic here is that the tilting of the enclosure from $\psi = 180°$ produces first a decrease and then an increase in the Nusselt number, and a local minimum value occurs at some critical angle ψ_c. Here ψ_c is about 174°, which is just the angle at which the multicell center moves to the $x = 2H$ plane, or at which the two-cell model in view A of Figure 4 changes to a unicell. This observation along with the observation that the local minimum Nusselt number happens at a transition of the 2-D multicell in the y-z plane to a 2-D unicell in the x-y plane for the transverse enclosure, and that at a transition of the 2-D multicell in the x-y plane to a unicell in the x-y plane for the longitudinal enclosure, leads to the conclusion that the generation of the 2-D unicell driven by hydrodynamic effects from any other flow pattern in tilted rectangular enclosures always implies a corresponding local minimum heat transfer rate. The Nusselt number dependence on the tilt angle in the range below the critical angle is really not much different from the one predicted by the two-dimensional model.

Bimodal flow with $A_x = A_z = 3.0$

For aspect ratios of $A_x = A_z = 3.0$, the situation is expected to be different in view of the reduced wall effect. Numerical calculations have been carried out with a uniform grid with $36 \times 12 \times 36$ cells ($n_x \times n_y \times n_z$, or $\Delta x = \Delta y = \Delta z = \frac{1}{12}H$) and the same Rayleigh number 8×10^3. The initial conditions used are the same as those for $A_x = A_z = 2.0$. The flow field at $\psi = 180°$ is shown in Figure 6(a). Seen from view B (top view) are four cells, and each cell is similar to that for $A_x = A_z = 2.0$. There are two surfaces on each cell which interact with other cells, and they appear as individual cells with two drag free and adiabatic surfaces. The flow field is a combination of four roll-cells with axes parallel to the x-axis and another four parallel to the z-axis. From the linear stability analysis of Davis[17] the model should have three cells in each direction. However, the symmetry of the geometry and initial conditions cannot produce this symmetrical model unless appropriate disturbances are introduced at the beginning. Attempts were not made to try to reproduce the 3×3 cell model but rather to see how this 4×4 mode behaves.

It is appropriate to point out that the multiple-cell model in the present case is not unique. Since the Rayleigh number is higher than critical, bifurcation can be expected. Here the initial conditions are expected to play an important role in the final solution. Calculations have been carried out by stretching the box from $A_x = A_z = 2.0$ to $A_x = A_z = 3.0$ with the initial conditions given by the stable flow of the 2×2 cell model. The resulting flow is still found to be that of the 2×2 cell model instead of the 4×4 cell model of the case when the initial conditions are that of pure conduction and no flow. It has also been found that as long as the 4×4 cell model is used as the initial condition, changes in the Rayleigh number from 4×10^3 to 3.2×10^4 do not affect the basic nature of the flow.

Geometrical influences on the transition from 4×4 to 2×2 or from 2×2 to 4×4 cells are not considered here. It is a bifurcation problem and will be discussed in another paper. Several numerical experiments with different aspect ratios between 2.0 and 3.0 show that the preferred mode is either 4×4 cells or 2×2 cells, and there is no other geometry at which both modes are possible or both modes are exchangeable. Comparing Figure 4(a) and Figure 6(a), we can find a totally different flow path in the central region: one is flowing up (2×2 cell), and the other is flowing down (4×4 cells). To switch the flow direction is not feasible, especially since each model is very stable. As could be predicted, the Nusselt number of 2.16 is higher than the one for $A_x = A_z = 2.0$.

This enclosure with $A_x = A_z = 3.0$ is now tilted to 2° from the horizontal plane or $\psi = 178°$. As seen from Figure 6(b) the cell far from the z-axis in view A is washed out, and the center of the four cells moves up, with two expanded and the other two constrained in shape when seen from view B, while the four cells in view C behave similarly to those in the transverse enclosure with two cells near the wall vanishing first. The process can really be classified as simultaneous transitions of those found in the longitudinal enclosure and the transverse enclosure.

At $\psi = 176°$ Figure 6(c), the four cells in view C are almost washed out, except that some images can still be observed along the center line of the two remaining cells. The enclosure acts more or less like a longitudinal enclosure with three nearly uniform roll-cells with axis parallel to the z-axis. This flow model remains the same until a tilt angle of 170°, Figure 6(d), is reached. At this angle the hydrodynamic force, which is proportional to $g \sin \psi$, aids the circulation of the two cells near the wall along $x = 0$ and A_x, and resists the circulation of the central cell, is sufficiently large to make the central cell reverse its

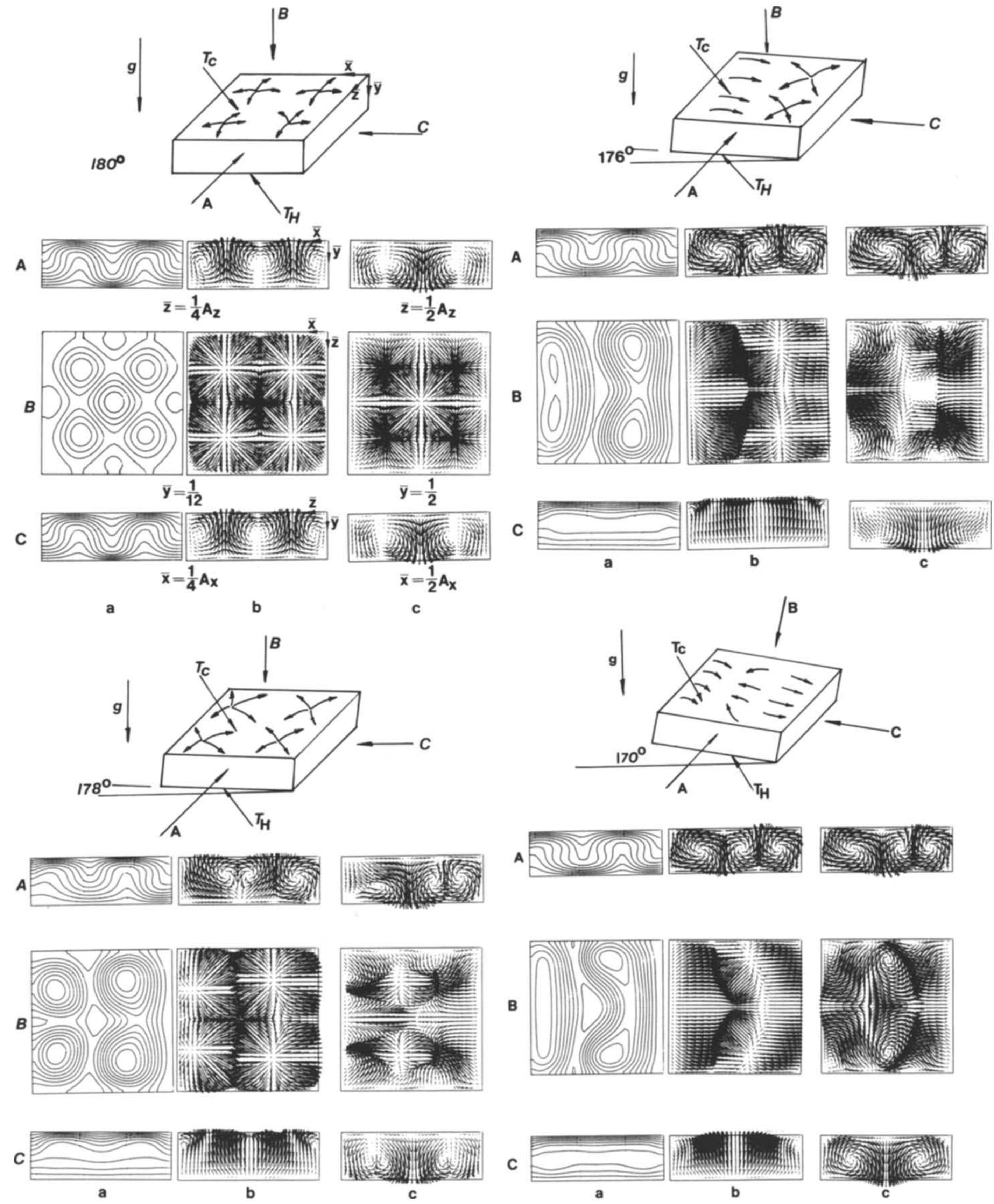

Figure 6 Isotherms a and flow patterns b, c in a tilted square box of $A_x = A_z = 3.0$ and $Ra = 8 \times 10^3$: (a) $\psi = 180°$; (b) $\psi = 178°$; (c) $\psi = 176°$; (d) $\psi = 170°$; (e) $\psi = 165°$; (f) $\psi = 160°$; (g) $\psi = 90°$

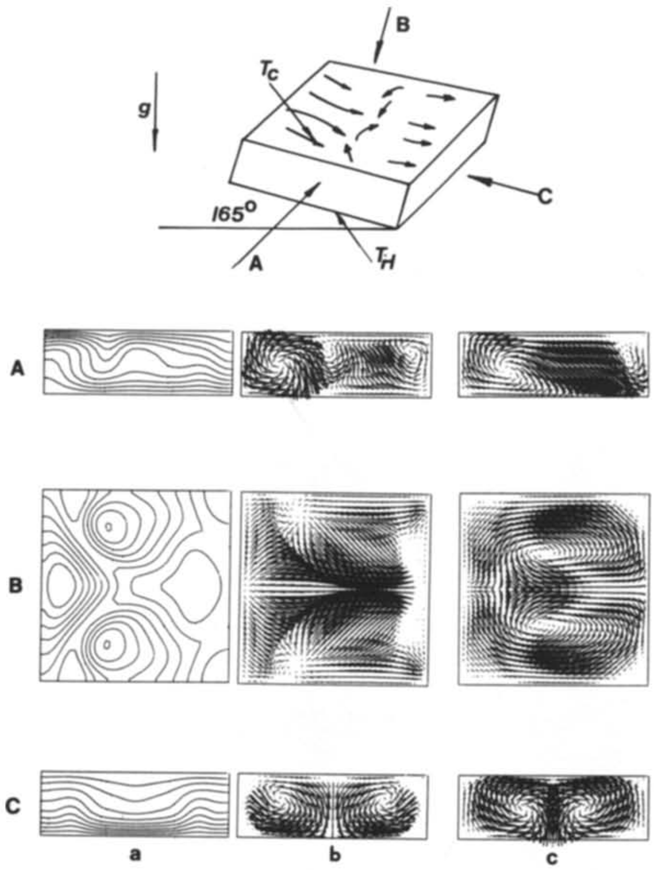

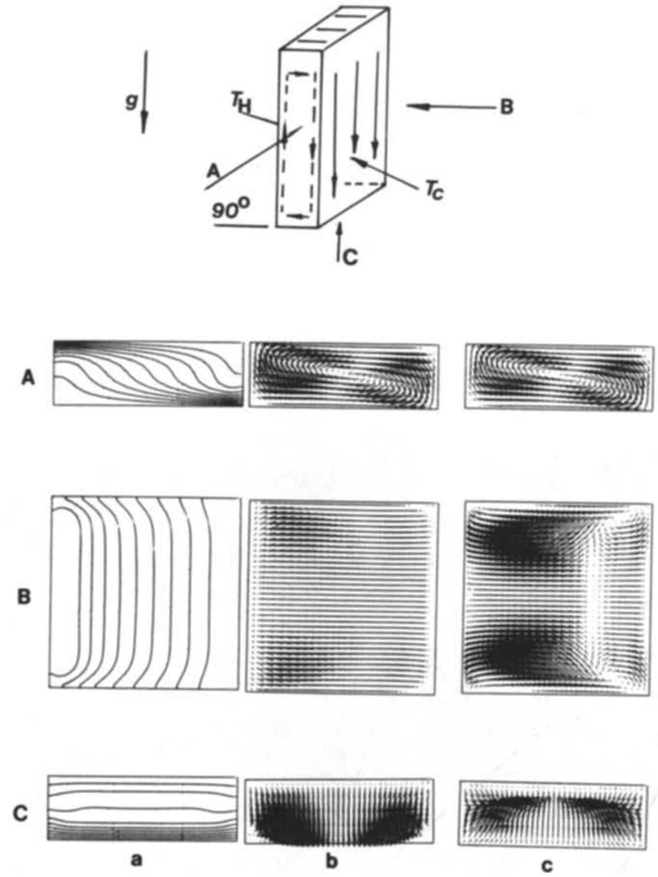

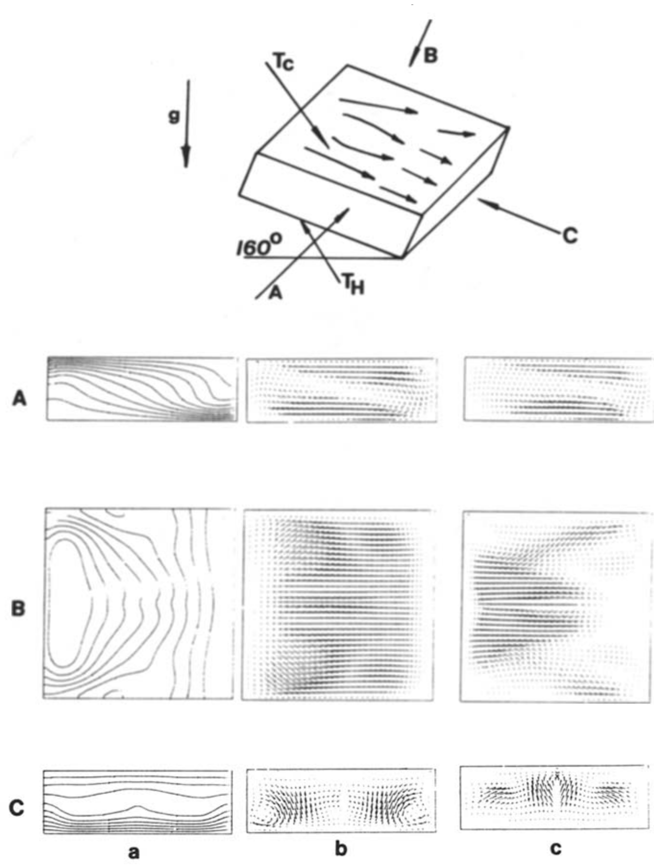

Figure 6 (continued)

flow. This process, which is three-dimensional as seen in the top view **B**, is such that the central cell switches its rotation axis 180° in the plane parallel to the isothermal surfaces. At $\psi = 170°$, it is inclined at 45°, at $\psi = 165°$ (Figure 6(e)) it is 90°, and at $\psi = 160°$ (Figure 6(f)) it turns to 180° to form a unicell. As a result of the change of the circulation axes of the central cell, the two cells in view C reappear between tilt angles 170° and 160° in the vicinity of $x = \frac{3}{2}H$. They finally disappear again as 160° is approached. Detailed calculations have been performed to track the vanishing process of the central cells, and this is shown by the schematic for the top view in Figure 7. This characteristic has also been found in our longitudinal enclosure studies.

The fluid behavior inside the enclosure at angles below the critical angle of 160° is essentially the same as that predicted by the two-dimensional model if the small influence on the third dimension lateral walls is ignored (see Figure 6(g) at $\psi = 90°$). The heat transfer behaves similarly to that of the $A_x = 2.0$ case, in that a local minimum occurs at a critical angle of 160° at which a unicell is formed, but this critical angle shows a dependence of ψ_c on the aspect ratio.

Conclusions

Based on this study the following conclusions can be made:

(1) When rectangular enclosures with equal aspect ratios A_x and A_z are heated from below, the flow patterns are the combination of two sets of rolls, which are perpendicular to each other.
(2) The number of the rolls in each direction for the heated-from-below case depends on the aspect ratio, when the flow

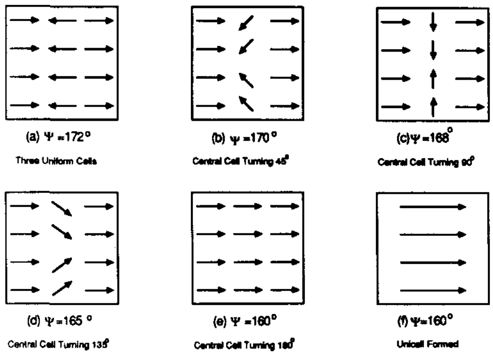

Figure 7 Illustration of the top view of the flow transition from three cells to one cell

field starts from rest. Once the bimodal motion is set up, the system is very stable and insensitive to the changes of Rayleigh number and aspect ratios.

(3) When the enclosure with $A_x = A_z$ is tilted from a multicell structure at 180°, the transition is basically the combination of those of transverse and longitudinal enclosures.

(4) In the bimodal flow the transition form of a longitudinal enclosure initiates at an angle closer to 180° when compared to that of a transverse enclosure. In the latter case, the roll-cells whose circulation is opposite to the buoyant force experience a rotation of 180° of the axis of circulation in a three-dimensional fashion.

(5) The Nusselt number for bimodal transition varies with the tilt angle in a similar way to those of longitudinal and transverse enclosures. A local minimum Nusselt number occurs at the angle where the complicated multicell patterns change to a unicell flow.

Acknowledgment

The authors wish to acknowledge the support of the National Science Foundation, under Grant CBT82-19158 to the University of Notre Dame, and the computing center of the University of Notre Dame.

References

1 Catton, I. Natural convection in enclosures. Proc. 6th Int. Heat Transfer Conf., Toronto, Hemisphere, Washington, D.C., 1978, **6**, 13–31

2 Ostrach, S. Natural convection heat transfer in cavity and cells. Proc. 7th Int. Heat Transfer Conf., München, Hemisphere, Washington, D.C., 1982, **1**, 365–379

3 Yang, K. T. Natural convection in enclosures. In: *Handbook of Single Phase Convective Heat Transfer*, eds. S. Kakac, R. K. Shah, and W. Aung, Wiley-Interscience, New York, 1987

4 Yang, K. T. and Lloyd, J. R. eds., Proc. Workshop on Natural Convection, National Science Foundation and University of Notre Dame, 1983

5 Yang, H. Q., Yang, K. T., and Lloyd, J. R. Flow transition in laminar buoyant flow in a three-dimensional tilted rectangular enclosure. Proc. 8th Int. Heat Transfer Conf., San Francisco, Hemisphere, Washington, D.C., 1986, **4**, 1495–1500

6 Yang, H. Q., Yang, K. T., and Lloyd, J. R. Laminar natural-convection flow transitions in tilted three-dimensional longitudinal rectangular enclosures. *Int. J. Heat Mass Transfer*, 1987, **30**, 1637–1644

7 Arnold, J. N., Catton, I., and Edwards, D. K. Experimental investigation of natural convection in inclined rectangular regions of differing aspect ratios. *J. Heat Transfer*, 1976, **98**, 67–71

8 Ozoe, H., Sayama, H., and Churchill, S. W. Natural convection in an inclined rectangular channel at various aspect ratio and angles—experimental measurements. *Int. J. Heat Mass Transfer*, 1975, **18**, 1425–1431

9 Schinkel, W. M. M. Natural convection in inclined air-filled enclosures. Dutch Efficiency Bureau-Pijnacker 15BN-90-6231-079-6, 1980

10 Ozoe, H., Fujii, K., Lior, N., and Churchill, S. W. Long roll generated by natural convection in an inclined rectangular enclosure. *Int. J. Heat Mass Transfer*, 1983, **26**, 1427–1438

11 Symons, J. G., and Peck, M. K. Natural convection heat transfer through inclined longitudinal slots. *J. Heat Transfer*, 1984, **106**, 824–829

12 Stork, K. and Müller, U. Convection in boxes: experiments. *J. Fluid Mech.*, 1970, **54**, 599–611

13 Leonard, B. P. A convectively stable, third-order accurate finite-difference method for steady two-dimensional flow and heat transfer. In: *Numerical Properties and Methodologies in Heat Transfer*, ed. T. M. Shih, Hemisphere, Washington, D.C., pp. 211–226, 1983

14 Yang, H. Q. Laminar buoyant flow transition in three-dimensional rectangular enclosures. Ph.D. thesis, University of Notre Dame, 1987

15 Ozoe, H., Yamamoto, K., Churchill, S. W., and Sayama, H. Three-dimensional, numerical analysis of laminar natural convection in a confined fluid heated from below. *J. Heat Transfer*, 1976, **98**, 202–207

16 Chan, A. M. C. and Banerjee, S. A numerical study of three-dimensional roll cells within rigid boundaries. *J. Heat Transfer*, 1979, **101**, 233–237

17 Davis, S. H. Convection in a box: linear theory. *J. Fluid Mech.*, 1967, **30**, 465–478